Research Article

Received: 2 March 2022 Revised: 3 August 2022 Accepted article published: 23 August 2022 Published online in Wiley Online Library: 8 September 2022

(wileyonlinelibrary.com) DOI 10.1002/ps.7145

RNAi of *Mannosidase-Ia* in the Colorado potato beetle and changes in the midgut and peritrophic membrane

Dongdong Liu,[a†] Kristof De Schutter,[a†] Johann Far,[b] An Staes,[c,d] Koen Dewettinck,[e] Loic Quinton,[b] Kris Gevaert[c,d] and Guy Smagghe[a*]

Abstract

Background: In addition to its role in the digestive system, the peritrophic membrane (PM) provides a physical barrier protecting the intestine from abrasion and against pathogens. Because of its sensitivity to RNA interference (RNAi), the notorious pest insect, the Colorado potato beetle (CPB, *Leptinotarsa decemlineata*), has become a model insect for functional studies. Previously, RNAi-mediated silencing of *Mannosidase-Ia* (*ManIa*), a key enzyme in the transition from high-mannose glycan moieties to paucimannose *N*-glycans, was shown to disrupt the transition from larva to pupa and the metamorphosis into adult beetles. While these effects at the organismal level were interesting in a pest control context, the effects at the organ or tissue level and also immune effects have not been investigated yet. To fill this knowledge gap, we performed an analysis of the midgut and PM in *ManIa*-silenced insects.

Results: As marked phenotype, the $ManIa^{RNAi}$ insects, the PM pore size was found to be decreased when compared to the control GFP^{RNAi} insects. These smaller pores are related to the observation of thinner microvilli (Mv) on the epithelial cells of the midgut of $ManIa^{RNAi}$ insects. A midgut and PM proteome study and reverse transcription quantitative polymerase chain reaction (RT-qPCR) analysis with a selection of marker genes was performed to characterize the midgut cells and understand their response to the silencing of *ManIa*. In agreement with the loss of *ManIa* activity, an accumulation of high-mannose *N*-glycans was observed in the *ManIa*-silenced insects. As a pathogen-associated molecular pattern (PAMP), the presence of these glycan structures could trigger the activation of the immune pathways.

Conclusion: The observed decrease in PM pore size could be a response to prevent potential pathogens to access the midgut epithelium. This hypothesis is supported by the strong increase in transcription levels of the anti-fungal peptide *drosomycin-like* in $ManIa^{RNAi}$ insects, although further research is required to elucidate this possibility. The potential immune response in the midgut and the smaller pore size in the PM shed a light on the function of the PM as a physical barrier and provide evidence for the relation between the Mv and PM.
© 2022 Society of Chemical Industry.

Supporting information may be found in the online version of this article.

Keywords: CPB; N-glycosylation; mannosidase-I; peritrophic membrane; microvilli; epithelial cells; defense; immune

1 INTRODUCTION

The insect gut is at the intersection between the organisms' immune defense and metabolic control. Aside from its central role in digesting and absorbing nutrients, the inner lining of the digestive tract is also an access point to a wide variety of pathogens. The peritrophic membrane (PM) is a non-cellular, semi-permeable structure lining the midgut and functions as a first line of defense preventing mechanical injuries and hindering or impeding the entry of pathogens, physical objects and large molecules or aggregates based on the pore size of the PM.[1–3] Traditionally, insect PMs are categorized as type I and type II according to their method of formation.[4] The coleopteran PM is a type I membrane and is secreted along the midgut by the columnar epithelial cells.[5–7] The PM is composed of chitin microfibrils and proteins, in which proteins account for 20–55% of the main PM mass and most of these are glycoproteins.[8,9] The characteristic properties

* *Correspondence to: Guy Smagghe, Laboratory of Agrozoology, Department Plants and Crops, Faculty of Bioscience Engineering, Ghent University, Ghent, Belgium. E-mail: guy.smagghe@ugent.be*

† *These authors contributed equally to this study.*

a *Laboratory of Agrozoology, Department Plants and Crops, Faculty of Bioscience Engineering, Ghent University, Ghent, Belgium*

b *Mass Spectrometry Laboratory, MolSys Research Unit, University of Liège, Liège, Belgium*

c *VIB Center for Medical Biotechnology, Ghent University, Ghent, Belgium*

d *Department of Biomolecular Medicine, Ghent University, Ghent, Belgium*

e *Food Structure and Function Research Group, Department of Food Technology, Safety and Health, Faculty of Bioscience Engineering, Ghent University, Ghent, Belgium*

of the PM, such as permeability and strength, are reported to be related to the composition of the proteins. Therefore, changes in the PM proteome may influence the PM structure, including the pore size, which may further influence its function as a physical barrier.

The midgut epithelium provides a selective, absorptive barrier between the lumen of the gut and the underlying tissues. It is the primary tissue for enzyme production and secretion.[10] The cell apex of the epithelial cells, which extends into the lumen of the gut, is specialized to form a regular array of uniform, straight structures, called microvilli (Mv), which increase the absorptive surface area of the connecting columnar cells. It is the direct site for food digestion, and nutrient absorption and it takes up the nutrients from the apical domain to transport them to the basolateral side for later distribution to the rest of the organism.[11] In addition, the Mv of the epithelial cells are required for the synthesis of the PM. It has long been proposed that the PM chitin network was molded upon the Mv.[9,12] This notion, that the Mv function as a template for PM network formation, is confirmed by the correlation between PM microfibril bundles and Mv diameter.[13] Later microscopic studies also showed that the PM delaminated from the Mv beneath.[14] When the chitin structure is interlocked, the Mv secrete protein into PM to form the protein components in PM.[15,16] Next to their role in food digestion, midgut epithelial cells play a crucial role in the insect defense system. As pathogens are mainly acquired through the oral route, the insect gut is at the front line acting as a physical barrier. In addition, these cells are also involved in the humoral response. The expression of pattern recognition receptors (PRRs) allows the detection of pathogens and the activation of local defenses, for example, anti-microbial peptides (AMPs).[17,18]

The Colorado potato beetle (CPB, *Leptinotarsa decemlineata* (Say), Coleoptera: Chrysomelidae), has received enormous attention due to its notorious impact on potato plants.[19] This beetle is well-suited to agricultural environments, and together with a remarkable adaptability to a variety of stressors and developed resistance against insecticides, these characteristics make CPB a very important pest.[20–23] Previously, characterization of the glycome of the PM glycoproteins in CPB revealed that paucimannose *N*-glycans dominate the PM glycome.[24] A key enzyme in the processing of high-mannose glycan structures, allowing the generation of paucimannose moieties, is *Mannosidase-Ia* (*ManIa*), which trims the $Man_9GlcNAc_2$ glycans down to $Man_5GlcNAc_2$ and this leads in turn to the production of paucimannose glycans.[16,25] Previously, the role of *ManIa* in survival, embryonic development and molting/metamorphosis of *Drosophila melanogaster*, *Tribolium castaneum*, *Nilaparvata lugens*, and *L. decemlineata* has been analyzed by RNA interference (RNAi)-mediated silencing,[16,26–30] but so far the effects on the midgut and PM have not been investigated.

Despite research into the structure and synthesis of the insect PM, the influence of internal or external perturbations on the structure of the PM is not studied enough. As one of the most important post-transcriptional modifications, here, the impact of manipulations in the N-glycosylation pathway on the structure of the PM was investigated. Therefore, the *ManIa*-activity was abolished by RNAi-mediated silencing, and the effects of the gene silencing on the structure of the PM were assessed by scanning electron microscopy (SEM). To further investigate the effects, the link between Mv and PM pores was also evaluated via SEM, and this analysis could also reveal a close relationship between the Mv and PM. To confirm that the observed phenotype of the Mv is induced and not the result of cell toxicity, a proteome study and quantitative polymerase chain reaction (qPCR) analysis with a selection of marker genes was performed. In agreement with a loss of *ManIa* activity, analysis of the glycan profile in $ManIa^{RNAi}$ insects by mass spectrometry (MS) revealed the accumulation of high-mannose glycans. As a potential pathogen-associated molecular pattern (PAMP), the activation of immune pathways by the high-mannose glycans was investigated by analyzing the transcription levels of immune-related genes. While *ManIa* was previously screened for effects on survival and development, revealing mortality in the transition from pupae in CPB and deformed wings in the $ManIa^{RNAi}$ insects,[29] the phenotype of *ManIa*-silencing in the midgut with a focus on immune response and physical defense was unexplored. Our new data contribute to the current knowledge of the role of N-glycosylation in the structure and function of the PM and provide evidence for the relation between the Mv and PM. In addition, our data support the hypothesis that silencing of *ManIa* in CPB may trigger an immune response in the midgut, leading to a decrease in Mv diameter size and subsequent smaller PM pores. Consequently, this change in pore size may enhance the PM's ability to limit the access of pathogens to the midgut epithelium, bolstering its function as a physical barrier.

2 MATERIALS AND METHODS

2.1 Insect rearing

A continuous colony of CPB was kept under standard rearing conditions on fresh potato foliage at 23 °C with 60% relative humidity and a 16 h light:8 h dark photoperiod at Ghent University, Belgium.[31] For the microinjection experiments, an appropriate amount of second instar CPB larvae were collected 0–12 h after molting to prepare a synchronized CPB population until they reached the third instar stage.

2.2 RNAi of *ManIa*: dsRNA synthesis and injection

Double-stranded RNA (dsRNA) targeting *ManIa* (Forward primer: GGCATACCTTAGCGACGTGA; Reverse primer: CATCCTGCTGAGGGTCTTCG) was synthesized using the MEGAscript™ RNAi Kit (catalog no. AM1626) (Invitrogen, Vilnius, Lithuania) according to the manufacturer's instructions using primers containing the T7 promoter sequence (TAATACGACTCACTATAGGGAGA). After elution of the dsRNAs in nuclease-free water, the concentration of dsRNA was measured by Nanodrop ND-1000 (NanoDrop Technologies, Wilmington, DE, USA) and the samples were diluted in nuclease-free water to 1.2 μg/μL. The quality was checked on a 1.5% agarose gel. Then, synchronized freshly molted third instar larvae of CPB larvae (0–3 h) with approximately same size and weight (18 ± 2.5 mg) were prepared for dsRNA injection. Each insect was injected with 400 nL of dsRNA at 1.2 μg/μL using a FemtoJet® injector (Eppendorf, Hamburg, Germany). Insects in the control group were injected with an equal 480 ng of dsGFP (green fluorescent protein) in the same volume, as described in Liu *et al.*[29]

Upon injection with dsRNA, the insects were scored for gene-silencing of the target gene (*ManIa*). This was performed by analyzing the transcription levels of the target gene relative to the control. The qPCR results were processed in qBase+. In addition, we followed the fresh insect body weight gain, survival and development of treated and control insects on a daily basis during the experiment of 4 days under normal feeding conditions.

© 2022 Society of Chemical Industry.

15264998, 2022, 12, Downloaded from https://onlinelibrary.wiley.com/doi/10.1002/ps.7145 by University of Liege Library Léon Graulich, Wiley Online Library on [11/05/2023]. See the Terms and Conditions (https://onlinelibrary.wiley.com/terms-and-conditions) on Wiley Online Library for rules of use; OA articles are governed by the applicable Creative Commons License

2.3 Dissection of PM and midguts and sample preparation for *N*-glycans, SEM, proteomics and qPCR analyses

At 4 days post-injection of dsRNA, PMs and midguts were dissected in chilled 4 °C phosphate-buffered saline (PBS) solution [140 mmol/L sodium chloride (NaCl), 1 mMmol/L potassium chloride (KCl), 6 mmol/L phosphate buffer, pH 7.4] for *N*-glycan analysis, SEM observation and qPCR analysis. For the proteome analysis, midguts were dissected at 3 days post-injection of the dsRNA. The insects were starved for 2 h before dissection, this was to limit the amount of food present in the intestine. During the dissection, the PM was removed from the gut and the midguts were washed several times in PBS solution to remove all food residues. Similar, for the analysis of the *N*-glycan profile of the PM and midgut, insects were starved for 2 h before dissection, and the collected PMs and midguts were washed in PBS solution several times before storage. For the SEM experiment, after washing in PBS, the dissected midgut tissues and PMs were fixed in 2.5% paraformaldehyde overnight and kept at 4 °C until further processing. For the proteome study, midguts were pooled after dissection and stored at −80 °C until protein extraction. For the qPCR analysis, the dissected midguts were stored at −80 °C until further processing.

2.4 *N*-Glycan profiling analysis of PM by permethylation and MALDI-MS

The procedure for *N*-glycan extraction was done as described previously.[16,28,32] In brief, extraction was performed in three biological replicates, and each replicate used approximately 100 mg of isolated PM and midgut material. Specifically, the isolated clean PMs and the pure midgut epithelium were crushed separately in liquid nitrogen and the homogenized material was dissolved in extraction buffer [4% sodium dodecyl sulfate (SDS), 50 mmol/L dithiothreitol (DTT) in 0.1 mol/L Tris–HCl, pH 7.8]. Extracts were processed using the filter-aided sample preparation (FASP) method.[32] In brief, the extracts were first lysed during 3 min in boiling water and 3 min sonication in an ultrasonic bath. After the lysis, the extracts were centrifuged at 16 000 × *g* for 15 min and the supernatant, containing the proteins were further purified by washing with 8 mol/L urea in 0.1 mol/L Tris–HCl pH 8.5 (UA) on Amicon Ultra 0.5 mL-centrifugal filters (30 kDa cut-off) (Millipore, Darmstadt, Germany). Quantification of the extract using the RC DC Protein Assay (Bio-Rad, Hercules, CA, USA) revealed a yield of about 10 mg proteins per 100 mg of PMs (wet). After four rounds of washes, proteins were alkylated prior to the addition of trypsin (Pierce, Thermo Fisher, Waltham, MA, USA). First, 50 mmol/L iodoacetamide was added to the UA solution and incubated in a thermo-mixer for 15 min at 37 °C. Then protein sample was washed twice with UA and twice with 40 mmol/L ammonium bicarbonate (ABC). Subsequently, trypsin was added in a ratio of 1:100 *w/w* (5 µg trypsin per 500 µg proteins per filter) and incubated at 37 °C with shaking for 18 h. Next, the tryptic peptides were collected in the supernatans after centrifugation at 14 000 × *g*. Peptide-*N*-glycosidaseA (PNGaseA; ProGlycAn, Vienna, Austria), in 100 µL of 50 mmol/L citrate–phosphate buffer (pH 5), was added to the reaction mixture and incubated overnight at 37 °C while shaking to release the *N*-glycans. Then, peptides were eliminated from the mixture by passing the mixture over a C18 cartridge (Waters, Milford, MA, USA) while collecting the eluent. Finally, the collected eluent containing the released *N*-glycans was dried under vacuum (SpeedVac SPD121P; Thermo Fisher).

The *N*-glycans fraction was derivatized by permethylation according to the protocol published in Smargiasso *et al.*[33] and adapted by Kang *et al.*[34] In brief, *N*-glycans were resuspended in 30 µL of dimethyl sulfoxide (DMSO) [containing a crushed bead of sodium hydroxide (NaOH)] and 20 µL of methyl iodide and the *N*-glycans were incubated for 30 min in glass tube under mild agitation. The samples were centrifuged at 1000 × *g*, and 20 µL of methyl iodide was added again and incubated again at room temperature for 20 min. The sample was centrifuged (1000 × *g*) before liquid–liquid extraction of the supernatant in water/chloroform of the permethylated *N*-glycans. The chloroform phase was collected and the samples were dried under vacuum (SpeedVac SPD121P; Thermo Fisher).

N-Glycan analysis was performed on an MALDI FT-ICR SolariX XR 9.4 T (Bruker, Bremen, Germany) mass spectrometer operating at *m/z* 300 to 3000 using resolving mass power [full width at half maximum (FWMH)] of approximately 200 000 at the *m/z* of the detected *N*-glycans. Each sample was spotted in triplicate by mixing 1 µL of diaminobenzophenone (10 mg/mL in 70% acetonitrile) and 1 µL of the sample resuspended in 70% acetonitrile, dried at room temperature and for each spot at least three mass spectra were recorded. Recorded mass spectra were processed using DataAnalysis 5.0 (Bruker) and assigned peaks were annotated against Glycoworkbench[35] and Expasy-GlycoMod tool (https://web.expasy.org/glycomod/) based on the glycans previously described in *D. melanogaster*, *T. castaneum* and *L. decemlineata*. The mass tolerance of the glycans was set at less than 0.2 Da for identification (typical mass accuracy was better than 2 ppm). Glycans identified with a larger mass error were excluded. *N*-Glycan structures were grouped into three main types: high mannose (Man(5–9), Man9Glc(1–3)), pauci-mannose (Man(2–4)), and hybrid and complex [containing at least one GlcNAc (*N*-acetylglucosamine) residue on the antennae] *N*-glycans. Differences in the *N*-glycan profile in the different treatments were analyzed using SPSS Statistics 24 [one way-analysis of variance (ANOVA) with least significant difference (LSD) test].

2.5 SEM of PM and Mv of midgut cells

After fixation in paraformaldehyde, the samples were post-fixed in 1% osmium tetroxide for 2 h, and then rinsed three times for 30 min with distilled water. Further, dehydration was accomplished with a sequence of ethanol solutions of increasing concentration (50%, 70% and 94% ethanol) for 30 min each. Subsequently, ethanol was replaced with acetone using an increasing concentration series (50%, 70% and 90%), each for 30 min. The samples were kept in acetone overnight, before being dried in a critical point dryer CPD 030 (Bel-tec, Balzers, Liechtenstein) with carbon dioxide (CO_2). The specimens were mounted on aluminum stubs with double-sided carbon tape and were sputter-coated with gold in a Jeol JFC-1300 auto sputter coater (JEOL, Tokyo, Japan). The analysis was completed using a JEOL JSF-7100F SEM as in Cagliari *et al.*[36] The dissections of PM and midgut were repeated three times with each time at least two PMs and midguts collected for structure observation. For the length and size calculation, at least two pictures were selected of each of the technical repeats. In each image, around 200 pores were selected for measurement. The size and width of the PM pores were analyzed in ImageJ (version 1.51). The length and width of each intact midgut microvillus (baseline to the apical Mv) were measured. Differences between PM pores size and Mv diameter in the different treatments were analyzed using SPSS Statistics 24 (one-way ANOVA, Kruskal–Wallis test).

© 2022 Society of Chemical Industry.

15264998, 2022, 12, Downloaded from https://onlinelibrary.wiley.com/doi/10.1002/ps.7145 by University of Liege Library Léon Graulich, Wiley Online Library on [11/05/2023]. See the Terms and Conditions (https://onlinelibrary.wiley.com/terms-and-conditions) on Wiley Online Library for rules of use; OA articles are governed by the applicable Creative Commons License

2.6 Proteome study of midgut

For protein extraction, the samples were basically processed as described in section 2.4 except that the extraction buffer was adjusted to 2% SDS, 50 mmol/L DTT in 0.1 mol/L Tris–HCl, pH 7.8. After trypsin digestion, around 2 mg peptides were collected using a two-time elution with 40 mmol/L ABC at 14 000 × *g* for 15 min and purified on C18 Ziptips (100 µL; Millipore) before liquid chromatography–tandem mass spectrometry (LC–MS/MS) analysis.

Proteome analysis was performed as described in Scheys *et al.*[37] Specifically, purified peptides were re-dissolved in 20 µL of loading solvent A [0.1% trifluoroacetic acid (TFA) in water/acetonitrile (98:2, *v/v*)] and for the shotgun experiments, the peptide concentration was determined on a Lunatic instrument (Unchained Lab, Pleasanton, CA, USA). For the shotgun experiments, an equivalent of 2 µg of peptide material was injected for LC–MS/MS analysis on an Ultimate 3000 RSLCnano ProFLow system in-line connected to a Fusion Lumos mass spectrometer (Thermo Fisher Scientific, Bremen, Germany). Trapping was performed at 10 µL/min for 4 min in loading solvent A on a 20 mm-trapping column (made in-house, 100 µm internal diameter (i.d.), 5 µm-diameter beads, C18 Reprosil-HD; Dr. Maisch, Ammerbuch, Germany). The peptides were separated on a 200 cm-µPAC™ column (C18-endcapped functionality, 300 µm wide channels, 5 µm porous-shell pillars, inter pillar distance of 2.5 µm and a depth of 20 µm; PharmaFluidics, Ghent, Belgium), kept at a constant temperature of 50 °C. In the case of the shotgun experiments, peptides were eluted by a linear gradient reaching 55% MS solvent B [0.1% formic acid (FA) in water/acetonitrile (2:8, *v/v*)] after 115 min and 99% MS solvent B at 120 min, followed by a 10 min wash at 99% MS solvent B and re-equilibration with MS solvent A (0.1% FA in water). The first 15 min the flow rate was set to 750 nL/min after which it was kept constant at 300 nL/min.

The mass spectrometer was for both sample sets operated in data-dependent mode, automatically switching between MS and MS/MS acquisition in TopSpeed mode. Full-scan MS spectra (300–1500 *m/z*) were acquired at a resolution of 120 000 in the Orbitrap analyzer after accumulation to a target automatic gain controller (AGC) value of 200 000 with a maximum injection time of 250 ms. The precursor ions were filtered for charge states (2–7 required), dynamic exclusion (60 s; ±10 ppm window) and intensity (minimal intensity of 3E4 count per scan). The precursor ions were selected in the ion routing multipole with an isolation window of 1.2 Th and accumulated to an AGC target of 5E3 or a maximum injection time of 40 ms and activated using HCD fragmentation at a normalized collision energy (NCE) of 34%. The fragments were analyzed in the ion trap analyzer at normal scan rate.

Data analysis was performed with MaxQuant (version 1.6.17.0) using the Andromeda search engine with default search settings, including a false discovery rate (FDR) set at 1% on both the peptide and protein level. Spectra were searched against the *L. decemlineata* proteome database, containing 18 499 sequences (https://i5k.nal.usda.gov/content/data-downloads) at the United States Department of Agriculture (downloaded March 2020). The mass tolerance for precursor and fragment ions was set to 4.5 and 20 ppm, respectively, during the main search. Enzyme specificity was set as C-terminal to arginine and lysine, also allowing cleavage at proline bonds with a maximum of two missed cleavages. Carbamidomethylation of cysteine residues was set as fixed modification. Variable modifications were set to oxidation of methionine residues and acetylation of protein N-termini. Matching between runs was enabled with a matching time window of 0.7 min and an alignment time window of 20 min. Only proteins with at least one unique or razor peptide (the group with the largest number of peptide IDs) were retained.

2.7 The qPCR analysis of midgut cells with selection of marker genes, including cell viability, proliferation, immune systems and responses, digestive enzymes

At 4 days post-injection of dsRNA, RNA was isolated from the midguts of the insects using the RNeasy® Mini Kit (Qiagen, Venlo, the Netherlands) according to the manufacturer's protocols. Three midguts were pooled together for each RNA extraction and the experiment was performed with three biological replicates for each treatment. The quantity and quality of the RNA were measured with a Nanodrop device (NanoDrop Technologies) and electrophoresis on a 1.5% agarose gel. The TURBO DNA-free Kit (Invitrogen) was used to remove genomic DNA from the total RNA samples. Subsequently, complementary DNA (cDNA) was synthesized from 2 µg of total RNA using the SuperScript® IV First-Strand cDNA Synthesis Reaction (Invitrogen) and diluted ten-fold for further analysis. Reverse transcription qPCR (RT-qPCR) was performed using a CFX96™ Real-Time PCR Detection system (BioRad, Nazareth, Belgium) with GoTaq® qPCR Master Mix (Promega, Madison, WI, USA). Each reaction was performed in triplicate (technical replicates). ARF and RP18 were used as reference genes. Stability of the reference genes and gene expression was analyzed using the qBase + software (Biogazelle, Ghent, Belgium). The primers used for the RT-qPCR reaction are listed in Supporting Information, Table S1. Statistical analyses were performed in the qBase + software (Biogazelle) and SPSS statistics 24 (Independent Samples *T*-test).

3 RESULTS

3.1 Silencing of *ManIa* has no effect on viability, growth and development of the insect

Injection of ds*ManIa* in third instar larvae of CPB resulted in silencing of the target gene expression of 80% (Fig. 1). In addition, it is to be noted that during the current experiments of 3–4 days, $ManIa^{RNAi}$ insects were normal since their survival (no mortality), development and weight gain were equal ($p > 0.05$) to the control insects treated with ds*GFP* (Fig. 1).

3.2 Silencing of *ManIa* leads to an accumulation in high-mannose *N*-glycans

ManIa is responsible for the trimming of high-mannose *N*-glycans and essential in the transition from high-mannose to paucimannose moieties. To analyze the impact of the down-expression of the *ManIa* on the glycan profile, *N*-glycans from the PM and midgut glycoproteome were isolated and analyzed by MS. The results showed a clear increase of two- and three-fold ($P < 0.01$, Student's *t*-test) in the relative abundance of high-mannose *N*-glycans in the PM and midgut, respectively, compared to the controls (Fig. 2). Correspondently, there was a respective two- and three-fold decrease in the relative abundance of paucimannose *N*-glycans ($P < 0.05$) (Fig. 2). For the hybrid- and complex *N*-glycans, no marked differences were observed in the PM and midgut between the GFP^{RNAi} and $ManIa^{RNAi}$ insects ($P > 0.05$).

 © 2022 Society of Chemical Industry.

15264998, 2022, 12, Downloaded from https://onlinelibrary.wiley.com/doi/10.1002/ps.7145 by University of Liege Library Léon Graulich, Wiley Online Library on [11/05/2023]. See the Terms and Conditions (https://onlinelibrary.wiley.com/terms-and-conditions) on Wiley Online Library for rules of use; OA articles are governed by the applicable Creative Commons License

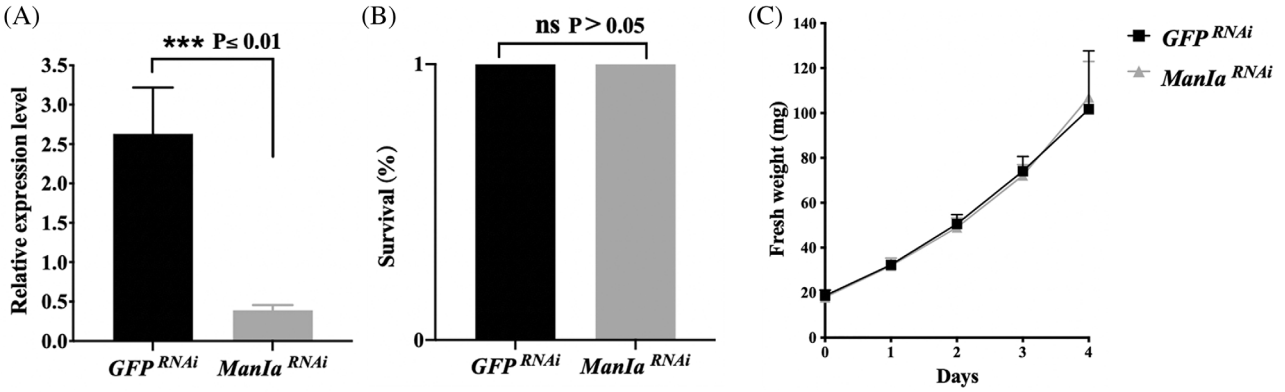

FIGURE 1. Silencing efficiency, viability, growth and development of *ManIa* ^{RNAi} and *GFP* ^{RNAi} insects. Data show the average of three biological repetitions ± standard deviation. (A) The relative expression level of *ManIa* in *GFP* ^{RNAi} and *ManIa* ^{RNAi} insects was 2.69 ± 0.59 and 0.39 ± 0.07, respectively, confirming a silencing efficiency of 80% at 4 days post-injection. (B) The survival rate (%) at 4 days post-injection in third instar larvae of Colorado potato beetle. ns represents no significant difference in survival between *ManIa* ^{RNAi} and *GFP* ^{RNAi} insects. (c) The fresh weight of insects (mg). There was no significant difference at every day (0–4) during the experiment in fresh weight (Independent samples *T*-test, *P* level 0.05).

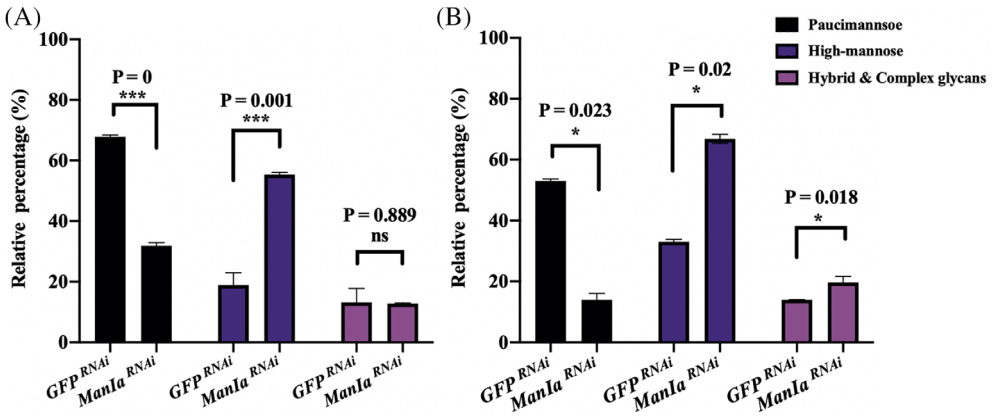

FIGURE 2. Glycan types in the peritrophic membrane (PM) and midgut cells (Mv) of *ManIa* ^{RNAi} and *GFP* ^{RNAi} insects. *N*-Glycan profiles in the PM (A) and midgut (B) of Colorado potato beetle larvae were determined 4 days after treatment with dsRNA targeting *ManIa* (*ManIa*^{RNAi}) or in control insects treated with dsRNA targeting *GFP* (*GFP*^{RNAi}). Bar graphs show the relative abundance (%) of different *N*-glycan groups; High-mannose, Paucimannose, and Hybrid & Complex *N*-glycans. Data are presented as the mean of three biological repeats per treatment. Each biological treatment consisted of three technical repeats with each three glycan MS spectra acquired. The relative abundance of glycans was analyzed by ANOVA and LSD *post hoc* test. Spectra are in Supporting Information, Fig. S1.

3.3 Silencing of *ManIa* causes a decrease in PM and Mv size

To investigate the effect of the decreased *ManIa* activity on the structure of the PM and Mv, dissected samples of the PM and midgut epithelium were visualized by SEM at 4 days after treatment with the dsRNA. Although the normal mesh structure of the PM was retained, the size of the pores in the PM of the *ManIa*^{RNAi} insects was significantly smaller (83 ± 2 nm) compared to 89 ± 1 nm in the *GFP*^{RNAi} controls (Kruskal–Wallis test, $P < 0.01$) (Fig. 3A,C,D). In agreement with the decrease in PM pore size, *ManIa*^{RNAi} insects showed Mv of the midgut epithelium with a smaller diameter (83 ± 2 nm) as compared to 87 ± 1 nm in the controls (Kruskal–Wallis test, $P < 0.01$) (Fig. 3B,E,F). In contrast, the length of the Mv was not affected (3760 ± 302 nm in *ManIa*^{RNAi} *versus* 3370 ± 86 nm in *GFP*^{RNAi} insects) ($P > 0.05$).

3.4 Proteome analysis of PM and midgut cells

The PM and midgut proteome was analyzed at 3 days after treatment with dsManIa and compared with the midgut proteome of the control insects (*GFP*^{RNAi}). In the midgut, a total of 1216 proteins were identified in *GFP*^{RNAi} insects and 1296 proteins in *ManIa*^{RNAi} insects (Table S2). The proteins were divided into several categories based on their function, including immune response, digestive process, cell structure, cell adhesion, neurogenesis and morphogenesis, metabolic process, transportation and transcription regulation. Hence, the gene ontology (GO) analysis on this midgut proteome revealed the presence of proteins linked to midgut functions (proteases and peptidases) (76 proteins) and insect immune pathway (43 proteins). Specifically, for the Toll immune pathway, we identified Dorsal (dl), a transcription factor involved in the expression of effector molecules, Spn88E, which negatively regulates the Toll signaling pathway and suppresses the expression of the antifungal peptide Drosomycin, and gd, which is involved in the stability of Spätzle, in the midgut of CPB (Table S2). In the PM, 269 proteins were identified in *GFP*^{RNAi} insects and 255 proteins in *ManIa*^{RNAi} insects (Table S3). The GO analysis on the PM proteome revealed a strong correlation with the midgut proteome. Indeed, there is a large overlap between the PM and midgut proteome, and the proteins of the PM were divided in the same categories as in midgut. Concerning the

 © 2022 Society of Chemical Industry.

15264998, 2022, 12, Downloaded from https://onlinelibrary.wiley.com/doi/10.1002/ps.7145 by University of Liege Library Léon Graulich, Wiley Online Library on [11/05/2023]. See the Terms and Conditions (https://onlinelibrary.wiley.com/terms-and-conditions) on Wiley Online Library for rules of use; OA articles are governed by the applicable Creative Commons License

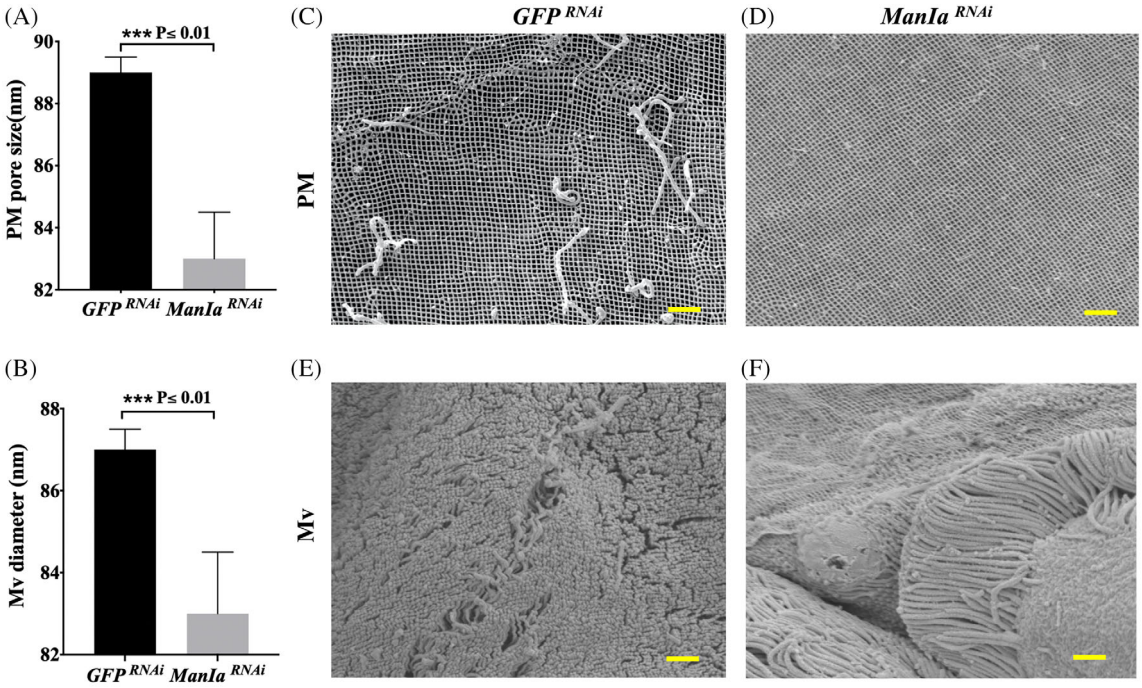

FIGURE 3. Structure of the peritrophic membrane (PM) and microvilli (Mv) of the midgut epithelium. Colorado potato beetle larvae were injected with dsRNA targeting *ManIa* or control treated with dsGFP. At 4 days post-treatment, the PM and midgut epithelium were dissected and visualized by SEM. PM pore size (A) and Mv tip diameter (B) (nm) were measured. Data are presented as mean ± standard deviation of three biological repeats per treatment. Each biological treatment consisted of at least two technical repeats. In each technical repeat, 200 PM pores or Mv diameters were measured. Statistical analysis was performed by non-parametric Kruskal–Wallis test. (C–F) SEM micrographs of the PM (C, D) and Mv (E, F) structure of *GFP* ^{RNAi} (C, E) and *ManIa* ^{RNAi} (D, F) insects. The scale bars are 1 μm.

immune-related proteins (14 proteins), in addition to the identification of Spn88E, also the Gram-negative bacteria-binding protein GNBP3, which acts as a PRR in the Toll immune pathway, was identified in the PM proteome (Table S3).

Of interest, when comparing the abundance of the identified proteins in the PM and midgut proteomes of *ManIa*^{RNAi} and *GFP*^{RNAi} insects, no significant differences were found (Table S2) (FDR 0.05, s0 0.1, Student's *t*-test, Perseus version 1.6.2.1).

3.5 The qPCR analysis of selected marker genes

To evaluate the physiological state of the midgut cells and further elucidate the mechanism behind the observed effects, the transcription levels of a selection of marker genes for the insect immune response, cell viability, cell proliferation, apoptosis-induction and digestion, as well as genes putatively involved in PM and Mv structure were analyzed in *GFP*^{RNAi} and *ManIa*^{RNAi} midgut samples (Table 1). Except for one gene, no up- or down-regulation of the transcription levels of these genes was observed in *ManIa*^{RNAi} insects when considering a cut-off value of two-fold regulation. Indeed, the transcription level of *drosomycin-like*, an anti-fungal and AMP gene of the Toll immune pathway, was found to be 2.8-fold (± 0.2) higher in *ManIa*^{RNAi} insects. In addition, it is worthy to mention that, although less than two-fold up-regulated, the transcript level of another Toll-pathway-related gene was increased. *Spätzle-processing enzyme* (*SPE*), coding for an enzyme upstream of *drosomycin-like* in the Toll-pathway, was found to be 1.7-fold (± 0.5) up-regulated in *ManIa*^{RNAi} midgut samples compared to controls (Table 1). Also of interest is the chloride channel protein (Clc-a), a Mv component, which was found to be down-regulated 0.56-fold (± 0.08). An analysis of potential glycosylation sites revealed that Clc-a has six potential N-X-S/T glycosylation sites.

4 DISCUSSION

Next to its evident role in the digestive system, the insect midgut is also an important organ in the defense against invading pathogens. While the separation of the intestinal lumen by the PM improves digestion efficiency by allowing efficient nutrient acquisition and reuse of hydrolytic enzymes,[8,38] this semi-permeable structure also provides a physical barrier to protect the midgut epithelium from toxins and pathogens.[3,38–44] Similarly, the Mv of the epithelial midgut cells do not only provide a structure for efficient absorption of nutrients and secretion of digestive enzymes, but also secrete AMPs and PM components.[45]

As a cell-free structure, all components of the PM must be secreted by the midgut epithelium. While the synthesis and structure of the PM remain not studied enough, it is expected that secretory vesicles release their cargo into the inter-Mv spaces. These components subsequently associate with the PM, which lies along the tips of the epithelial cell Mv.[46] This is in agreement with our SEM images showing the PM is lining with the tips of the Mv and our observation that the diameter of the Mv tips is equal to the size of the PM pores. Interestingly, in CPB, RNAi-mediated silencing of *ManIa*, coding for an enzyme in the N-glycosylation pathway essential in the transition from high-mannose to paucimannose glycans, led to a smaller pore size of the PM compared to control insects. Although there was a decrease in pore size, the PM showed a normal sieve structure. Analysis of the Mv morphology revealed that the smaller size of the PM pores in the *ManIa*-silenced insects agrees with a significant decrease in the

 © 2022 Society of Chemical Industry.

15264998, 2022, 12, Downloaded from https://onlinelibrary.wiley.com/doi/10.1002/ps.7145 by University of Liege Library Léon Graulich, Wiley Online Library on [11/05/2023]. See the Terms and Conditions (https://onlinelibrary.wiley.com/terms-and-conditions) on Wiley Online Library for rules of use; OA articles are governed by the applicable Creative Commons License

TABLE 1. Quantitative polymerase chain reaction (qPCR) analysis of transcription levels of marker genes at 4 days post-injection in $ManIa^{RNAi}$ insects compared to the controls (GFP^{RNAi})

Pathways	Gene name	Gene	FC ± standard error of the mean
Immune system	GNBP1	XM_023162103.1	1.00 ± 0.05
	PGRP-SA	XM_023170378.1	0.81 ± 0.20
	ModSP	XM_023162803.1	1.15 ± 0.42
	SPE (Spätzle-processing enzyme)	XM_023169799.1	1.67 ± 0.54
	Toll receptors 5	XM_023158765.1	1.05 ± 0.03
	Toll-9	XM_023168798.1	1.04 ± 0.05
	PGRP-LC	XM_023165651.1	1.07 ± 0.02
	Relish (Rel)	XM_023174540.1	1.09 ± 0.05
-Imd AMPs	Icarapin-like	XM_023157314.1	0.96 ± 0.38
	Acaloleptin A-like	XM_023174117.1	1.67 ± 0.62
	DIAP2	XM_023166533.1	1.08 ± 0.19
	Lysozyme-like	XM_023158986.1	1.38 ± 0.04
	Lysozyme-like	XM_023172373.1	1.53 ± 0.29
	Metchnikowin	XM_023170211.1	1.33 ± 0.39
	Drosocin	XM_023172078.1	0.90 ± 0.01
	Attacin-B-like	XM_023168856.1	0.65 ± 0.04
-Toll AMPs	Drosomycin-like	XM_023167050.1	2.82 ± 0.22
	Cactus-like	XM_023173411.1	1.34 ± 0.02
	NF-kappa-B inhibitor cactus-like	XM_023159220.1	1.09 ± 0.01
	Tube/Pelle	XM_023159822.1	1.05 ± 0.01
	dMyd88	XM_023155893.1	0.81 ± 0.05
Apoptosis	Caspase-like	XM_023172458.1	1.25 ± 0.23
	Capspase8	XM_023169721.1	1.12 ± 0.10
	P53	XM_023169112.1	0.97 ± 0.08
ISCs proliferation	HR3(20-hydroxyecdysone responsive gene)	KP340509.1	0.70 ± 0.14
	JH (juvenile hormone) response gene	XM_023163152.1	0.82 ± 0.16
	CyclinB	XM_023159762.1	0.75 ± 0.03
	CyclinE	XM_023171219.1	0.98 ± 0.12
	α-arylphorin	XM_023162016.1	1.17 ± 0.33
Microvilli structure	Ataxin-2 isoform	XM_023157140.1	0.93 ± 0.16
	Pez isoform A	XM_023166328.1	0.95 ± 0.34
	Ankyrin 2 isoform Q	XM_023163343.1	1.04 ± 0.25
	Ankyrin 2 isoform X	XM_023163344.1	0.94 ± 0.16
	Cuticular protein 62Bc isoform A	XM_023156264.1	0.82 ± 0.01
Apical part of the cell	Rush	XM_023156443.1	1.14 ± 0.18
	Wat	XM_023160758.1	1.03 ± 0.24
	Pde6	XM_023169322.1	1.10 ± 0.74
	Clc-a	XM_023162635.1	0.56 ± 0.08
Major peritrophins	Peritrophin-44	XM_023159685.1	0.52 ± 0.11
	Peritrophin-30	MF612053.1	1.10 ± 0.20
Digestive enzymes	Trypsin like	XM_023159521.1	1.21 ± 0.15
	Aspartic protease	XM_023156956.1	1.30 ± 0.92
	Cathepsin B	XM_023170019.1	1.31 ± 0.12
	Aminopeptidase	XM_023167900.1	1.04 ± 0.05

Note: The column FC ± standard error of the mean represents fold change (genes relative expression level in $ManIa^{RNAi}$ insects to GFP^{RNAi} ones). The experiment was done twice, and each time three biological repeats were performed and for each repeat, three midguts were pooled. The qPCR analysis was performed with two technically repeated measurements of each sample. Description of the genes: GNBP1 abbreviation of Gram-negative bacteria-binding protein 1; PGRP-SA abbreviation of peptidoglycan-recognition protein SA precursor; ModSP abbreviation of modular serine protease; SPE abbreviation of Spätzle-processing enzyme; PGRP-LC abbreviation of peptidoglycan-recognition protein LC; Relish (Rel) abbreviation of nuclear factor NF-kappa-B p110; DIAP2 abbreviation of death-associated inhibitor of apoptosis 2; Cactus-like abbreviation of NF-kappa-B inhibitor cactus-like; HR3 abbreviation of Probable nuclear hormone receptor HR3.Rush: name of pleckstrin homology domain-containing family F member 1 homolog protein. Wat: name of Fatty acyl-CoA reductase wat protein. Pde6c: name of GMP-specific 3′,5′-cyclic phosphodiesterase. Clc-a: name of chloride channel protein 2.

Mv diameter compared to the control insects. The resulting equal size of the PM pores and the Mv tips confirms the correlation between Mv diameter and PM pore size. Important to notice is that while the morphology of the Mv has changed after silencing of *ManIa*, the midgut epithelial cells remain normal and viable. This was confirmed by a proteome study of the midgut and PM

© 2022 Society of Chemical Industry.

15264998, 2022, 12, Downloaded from https://onlinelibrary.wiley.com/doi/10.1002/ps.7145 by University of Liege Library Léon Graulich, Wiley Online Library on [11/05/2023]. See the Terms and Conditions (https://onlinelibrary.wiley.com/terms-and-conditions) on Wiley Online Library for rules of use; OA articles are governed by the applicable Creative Commons License

and qPCR analysis on a selection of marker genes including markers for cell viability, apoptosis and cell proliferation, and digestive enzymes in midgut epithelial cells. This indicates that the observed morphological changes are not due to a cytotoxic response.

In accordance with a decreased *ManIa* activity, the glycome of *ManIa*^{RNAi} insects showed a significant accumulation of high-mannose glycans. High-mannose structures are present on the surface of many pathogens, and especially fungi decorate their glycoproteins with hyper-mannosylated glycans.[47] In turn, these structures can be recognized as PAMPs by PRRs, for example, mannose-binding lectin receptor.[18] In this project, we believe that this accumulation of high-mannose structures in the insect gut upon RNAi of *ManIa* can act as a PAMP and subsequently induce an immune response in the midgut epithelial cells. Therefore, we hypothesized that the PM structure can be adapted upon detection of pathogens, such as fungi, and that the observed changes in structure and morphology of the PM and Mv could be a response to the activation of the immune pathway in the insect. To support this hypothesis that the increase in high-mannose structures can function as an elicitor to activate the immune pathway in *ManIa*^{RNAi} insects, we investigated the transcript levels (qPCR analysis; Table 1) of several marker genes of the Toll immune pathway, including PRRs and AMPs, and also our proteome study (using the annotated proteins; Table S2 and S3) confirmed the presence of elements of this pathway both in the epithelial cells of the midgut of CPB and the PM. Interestingly, we observed a clear up-regulation of *drosomycin-like*, a typical anti-fungal AMP, and an increased expression of upstream Toll-related *SPE*, confirming that the Toll immune pathway is activated in *ManIa*^{RNAi} insects. The decrease in pore size of the PM could thus be a protective response to prevent potential pathogens to cross the PM into the ectoperitrophic space. However, before claiming solid conclusions, future experiments wherein high-mannose structures and fungi as a model for pathogen infection are introduced in the insect midgut, are necessary to confirm this induction of the insect immune system by the high-mannose glycans and the subsequent reduction in PM pore size.

Of interest, in relation to the Mv morphology, is the decreased expression of the chloride channel protein Clc-a. The potential of Clc-a to influence Mv morphology was reported in mice where a knockout of CLC-2, a Clc-a ortholog, resulted in disorganized, disrupted or even absent Mv.[48,49] It is therefore possible that a reduction in Clc-a levels in the *ManIa*^{RNAi} insects resulted in the observed decrease in Mv diameter. Whether the reduction in Clc-a levels is due to an activation of the immune pathway still needs to be confirmed.

5 CONCLUSION

In conclusion, a decrease in Mv diameter was observed upon RNAi-mediated silencing of *ManIa*. As PM synthesis is linked to the Mv tips, the decrease in Mv diameter correlates with a decrease in PM pore size. We speculate this decrease could be linked to an immune response triggered by the abundant presence of high-mannose *N*-glycans in *ManIa*^{RNAi} insects. The increased transcript levels of the anti-fungal AMP *drosomycin-like* are clear indications of this hypothesis, although further research is required to elucidate this possibility.

ACKNOWLEDGEMENTS

Dongdong Liu is the recipient of a doctoral grant provided by China Scholarship Council. This research was supported by the Research Foundation-Flanders (FWO-Vlaanderen, Belgium) and the Special Research Fund from the Ghent University (Belgium). The authors also thank Bart De Pauw (Ghent University), Benny Lewille (Ghent University), Mathieu Tiquet (University of Liège), Nanou Tanteliarisoa (University of Liège) for their respective help with the critical point drying, SEM, and glycan sample preparation and MALDI mass spectra acquisition. The MALDI/ESI dual source FT-ICR solariX XR 9.4 T was co-funded by FEDER BIOMED HUB Technology Support (number 2.2.1/996).

CONFLICT OF INTEREST

The authors declare no competing financial interest.

DATA AVAILABILITY STATEMENT

The data that support the findings of this study are available from the corresponding author upon reasonable request.

SUPPORTING INFORMATION

Supporting information may be found in the online version of this article.

REFERENCES

1 Tellam RL, The peritrophic matrix, in *Biology of the Insect Midgut*, ed. by Lehane MJ and Billingsley PF. Springer, Dordrecht, pp. 86–114 (1996).
2 Terra WR, The origin and functions of the insect peritrophic membrane and peritrophic gel. *Arch Insect Biochem Physiol* **47**:47–61 (2001).
3 Erlandson MA, Toprak U and Hegedus DD, Role of the peritrophic matrix in insect-pathogen interactions. *J Insect Physiol* **117**:103894 (2019).
4 Wigglesworth VB, Memoirs: the formation of the peritrophic membrane in insects, with special reference to the larvae of mosquitoes. *J Cell Sci* **2**:593–616 (1930).
5 Waterhouse DF, Digestion in insects. *Annu Rev Entomol* **2**:1–18 (1957).
6 Peters W, Occurrence of peritrophic membranes, in *Peritrophic Membranes*, ed. by Peters W. Springer, Berlin, Heidelberg, pp. 5–30 (1992).
7 Hopkins TL and Harper MS, Lepidopteran peritrophic membranes and effects of dietary wheat germ agglutinin on their formation and structure. *Arch Insect Biochem Physiol* **47**:100–109 (2001).
8 Hegedus D, Erlandson M, Gillott C and Toprak U, New insights into peritrophic matrix synthesis, architecture, and function. *Annu Rev Entomol* **54**:285–302 (2009).
9 Lehane MJ, Peritrophic matrix structure and function. *Annu Rev Entomol* **42**:525–550 (1997).
10 Lehane M and Billingsley P, in *Structure and Ultrastructure of the Insect Midgut, Biology of the Insect Midgut*, ed. by Lehane M and Billingsley P. Springer Science & Business Media, Dordrecht, pp. 3–30 (2012).
11 Caccia S, Casartelli M and Tettamanti G, The amazing complexity of insect midgut cells: types, peculiarities, and functions. *Cell Tissue Res* **377**:505–525 (2019).
12 Mercer EH and Day MF, The fine structure of the peritrophic membranes of certain insects. *Biol Bull* **103**:384–394 (1952).
13 Harper MS and Hopkins TL, Peritrophic membrane structure and secretion in European corn borer larvae (*Ostrinia nubilalis*). *Tissue Cell* **29**: 463–475 (1997).
14 Peters W, Heitmann S and D'Haese J, Formation and fine structure of peritrophic membranes in the earwig, *Forficula auricularia* (Dermaptera: Forficulidae) msrec: 1978-11-01. *Entomol Gen* **5**:241–254 (1979).
15 Bolognesi R, Ribeiro AF, Terra WR and Ferreira C, The peritrophic membrane of *Spodoptera frugiperda*: secretion of peritrophins and role in immobilization and recycling digestive enzymes. *Arch Insect Biochem Physiol* **47**:62–75 (2001).
16 Walski T, De Schutter K, Van Damme EJM and Smagghe G, Diversity and functions of protein glycosylation in insects. *Insect Biochem Mol Biol* **83**:21–34 (2017).

© 2022 Society of Chemical Industry.

15264998, 2022, 12, Downloaded from https://onlinelibrary.wiley.com/doi/10.1002/ps.7145 by University of Liege Library Léon Graulich, Wiley Online Library on [11/05/2023]. See the Terms and Conditions (https://onlinelibrary.wiley.com/terms-and-conditions) on Wiley Online Library for rules of use; OA articles are governed by the applicable Creative Commons License

17 Janeh M, Osman D and Kambris Z, Damage-induced cell regeneration in the midgut of *Aedes albopictus* mosquitoes. *Sci Rep* **7**:1–10 (2017).
18 Chen P, De Schutter K, Pauwels J, Gevaert K, Van Damme EJM and Smagghe G, Binding of *Orysata* lectin induces an immune response in insect cells. *Insect Sci* **29**:717–729 (2022).
19 Hare JD, Ecology and management of the Colorado potato beetle. *Annu Rev Entomol* **35**:81–100 (1990).
20 Alyokhin A, Baker M, Mota-Sanchez D, Dively G and Grafius E, Colorado potato beetle resistance to insecticides. *Am J Potato Res* **85**:395–413 (2008).
21 Alyokhin A, Colorado potato beetle management on potatoes: current challenges and future prospects. *Fruit Veg Cereal Sci Biotech* **3**:10–19 (2009).
22 Alyokhin A, Rondon S and Yulin G eds, *Insect Pests of Potato: Global Perspectives on Biology and Management*. Academic Press, San Diego (2022).
23 Schoville SD, Chen YH, Andersson MN, Benoit JB, Bhandari A, Bowsher JH *et al*., A model species for agricultural pest genomics: the genome of the Colorado potato beetle, *Leptinotarsa decemlineata* (Coleoptera: Chrysomelidae). *Sci Rep* **8**:1–18 (2018).
24 Liu D, De Schutter K, Smargiasso N, De Pauw E, Van Damme EJM and Smagghe G, The N-glycan profile of the peritrophic membrane in the Colorado potato beetle larva (*Leptinotarsa decemlineata*). *J Insect Physiol* **115**:27–32 (2019).
25 Kawar Z and Jarvis DL, Biosynthesis and subcellular localization of a lepidopteran insect alpha 1, 2-mannosidase. *Insect Biochem Mol Biol* **31**:289–297 (2001).
26 Kerscher S, Albert S, Wucherpfennig D, Heisenberg M and Schneuwly S, Molecular and genetic analysis of the *Drosophila* mas-1 (mannosidase-1) gene which encodes a glycoprotein processing α1, 2-mannosidase. *Dev Biol* **168**:613–626 (1995).
27 Rosenbaum EE, Vasiljevic E, Brehm KS and Colley NJ, Mutations in four glycosyl hydrolases reveal a highly coordinated pathway rhodopsin biosynthesis and N-glycan trimming in *Drosophila melanogaster*. *PLoS Genet* **10**:e1004349 (2014).
28 Walski T, Van Damme EJM, Smargiasso N, Christiaens O, De Pauw E and Smagghe G, Protein N-glycosylation and N-glycan trimming are required for postembryonic development of the pest beetle *Tribolium castaneum*. *Sci Rep* **6**:1–15 (2016).
29 Liu D, De SK, Chen P and Smagghe G, The N-glycosylation-related genes as potential targets for RNAi-mediated pest control of the Colorado potato beetle (*Leptinotarsa decemlineata*). *Pest Manag Sci* **78**: 3815–3822 (2021). https://doi.org/10.1002/ps.6732.
30 Yang Q, De Schutter K, Chen P, Van Damme EJM and Smagghe G, RNAi of the N-glycosylation-related genes confirms their importance in insect development and α-1,6-fucosyltransferase plays a role in the ecdysis event for the Hemimetabolous pest insect *Nilaparvata lugens*. *Insect Sci* **29**:91–99 (2022).
31 Smagghe G, Eelen H, Verschelde E, Richter K and Degheele D, Differential effects of nonsteroidal ecdysteroid agonists in Coleoptera and Lepidoptera: analysis of evagination and receptor binding in imaginal discs. *Insect Biochem Mol Biol* **26**:687–695 (1996).
32 Scheys F, De Schutter K, Shen Y, Yu N, Smargiasso N, De Pauw E *et al*., The N-glycome of the hemipteran pest insect *Nilaparvata lugens* reveals unexpected sex differences. *Insect Biochem Mol Biol* **107**: 39–45 (2019).
33 Smargiasso N, Nader J, Rioux S, Mazzucchelli G, Boutry M, De Pauw E *et al*., Exploring the N-glycosylation profile of glycoprotein B from human cytomegalovirus expressed in CHO and Nicotiana tabacum BY-2 cells. *Int J Mol Sci* **20**:3741 (2019).
34 Kang P, Mechref Y and Novotny MV, High-throughput solid-phase permethylation of glycans prior to mass spectrometry. *Rapid Commun* **22**:721–734 (2008).
35 Ceroni A, Maass K, Geyer H, Geyer R, Dell A and Haslam SM, GlycoWorkbench: a tool for the computer-assisted annotation of mass spectra of glycans. *J Proteome Res* **7**:1650–1659 (2008).
36 Cagliari D, Taning CNT, Christiaens O, De Schutter K, Lewille B, Dewettinck K *et al*., Parental RNA interference as a tool to study genes involved in rostrum development in the Neotropical brown stink bug. *Euschistus heros J Insect Physiol* **128**:104161 (2021).
37 Scheys F, Van Damme EJM, Pauwels J, Staes A, Gevaert K and Smagghe G, N-glycosylation site analysis reveals sex-related differences in protein N-glycosylation in the rice brown planthopper (*Nilaparvata lugens*). *Mol Cell Proteomics* **19**:529–539 (2020).
38 Bolognesi R, Terra WR and Ferreira C, Peritrophic membrane role in enhancing digestive efficiency theoretical and experimental models. *J Insect Physiol* **54**:1413–1422 (2008).
39 Levy SM, Falleiros ÂM, Moscardi F and Gregório EA, The role of peritrophic membrane in the resistance of *Anticarsia gemmatalis* larvae (Lepidoptera: Noctuidae) during the infection by its nucleopolyhedrovirus (AgMNPV). *Arthropod Struct Dev* **40**:429–434 (2011).
40 Weiss BL, Savage AF, Griffith BC, Wu Y and Aksoy S, The peritrophic matrix mediates differential infection outcomes in the tsetse fly gut following challenge with commensal, pathogenic and parasitic microbes. *J Immunol* **193**:773–782 (2014).
41 Shibata T, Maki K, Hadano J, Fujikawa T, Kitazaki K, Koshiba T *et al*., Crosslinking of a peritrophic matrix protein protects gut epithelia from bacterial exotoxins. *PLoS Pathog* **11**:e1005244 (2015).
42 Sadlova J, Homola M, Myskova J, Jancarova M and Volf P, Refractoriness of *Sergentomyia schwetzi* to *Leishmania spp*. is mediated by the peritrophic matrix. *PLoS Negl Trop Dis* **12**:e0006382 (2018).
43 Aksoy S, Tsetse peritrophic matrix influences for trypanosome transmission. *J Insect Physiol* **118**:103919 (2019).
44 Guo W, Kain W and Wang P, Effects of disruption of the peritrophic membrane on larval susceptibility to Bt toxin Cry1Ac in cabbage loopers. *J Insect Physiol* **117**:103897 (2019).
45 Merzendorfer H, Kelkenberg M and Muthukrishnan S, Peritrophic Matrices, in *Extracellular Composite Matrices Arthropods*, ed. by Cohen E and Moussian B. Springer, Cham, pp. 255–324 (2016).
46 Eisemann C, Wijffels G and Tellam RL, Secretion of the type 2 peritrophic matrix protein, peritrophin-15, from the cardia. *Arch Insect Biochem Physiol* **47**:76–85 (2001).
47 De Pourcq K, De Schutter K and Callewaert N, Engineering of glycosylation in yeast and other fungi: current state and perspectives. *Appl Microbiol Biotechnol* **87**:1617–1631 (2010).
48 Chuang JZ, Milner TA, Zhu M and Sung CH, A 29 kDa intracellular chloride channel p64H1 is associated with large dense-core vesicles in rat hippocampal neurons. *J Neurosci* **19**:2919–2928 (1999).
49 Hanke-Gogokhia C, Lehmann GL, Benedicto I, De la Fuente-Ortega E, Arshavsky VY, Schreiner R *et al*., Apical CLC-2 in retinal pigment epithelium is crucial for survival of the outer retina. *FASEB J* **35**:e21689 (2021).

 © 2022 Society of Chemical Industry.

15264998, 2022, 12, Downloaded from https://onlinelibrary.wiley.com/doi/10.1002/ps.7145 by University of Liege Library Léon Graulich, Wiley Online Library on [11/05/2023]. See the Terms and Conditions (https://onlinelibrary.wiley.com/terms-and-conditions) on Wiley Online Library for rules of use; OA articles are governed by the applicable Creative Commons License